Author Manuscript

Author Manuscript

Author Manuscript

Author Manuscript

HHS Public Access

Author manuscript

Methods Mol Biol. Author manuscript; available in PMC 2018 December 28.

Published in final edited form as:

Methods Mol Biol. 2013 ; 1042: 47–60. doi:10.1007/978-1-62703-526-2_4.

Measuring Transcription Dynamics in Living Cells using Fluctuation Analysis

Matthew L. Ferguson and **Daniel R. Larson***

Center for Cancer Research, National Cancer Institute, National Institutes of Health Bethesda, MD 20892

Summary

Single-cell studies of gene regulation suggest that transcription dynamics play a fundamental role in determining expression heterogeneity within a population. In addition, the three-dimensional organization of the nucleus seems to both reflect and influence expression patterns in the cell. Therefore, to gain a holistic understanding of transcriptional regulation, it is necessary to develop methods for studying transcription of single genes in living cells with high spatial and temporal resolution. In this chapter, we describe a recently-developed approach for visualizing and quantifying pre-mRNA synthesis at a single active gene in the nucleus. The approach is based on the high-affinity interaction between MS2 / PP7 bacteriophage coat proteins and RNA hairpins which are transcribed by the gene of interest. The MS2/PP7 coat protein is fused to a fluorescent protein and binds the nascent mRNA, allowing for detection of single transcription events in the fluorescence microscope. By time lapse fluorescence imaging and quantitative image analysis one can generate a time trace of fluorescence intensity at the site of transcription. By temporal autocorrelation analysis one can determine enzymatic activities of RNAP such as initiation rate and elongation rate. In this protocol, we summarize the experimental concept, design and execution for real-time observation of transcription in living cells.

Keywords

Fluorescence Fluctuation Spectroscopy; Fluorescence Correlation Spectroscopy; FCS; transcription; MS2; PP7; single-molecule; imaging; RNA; stochastic

1. Introduction

In recent years, live-cell microscopy in the nucleus has revealed previously unanticipated aspects of gene regulation. Chromatin-binding proteins show a surprising degree of dynamic mobility, with dwell times on the order of seconds[1]. Chromatin itself shows conformational fluctuations over several microns [2, 3]. Genes re-position within the nucleus in response to activation and inactivation [4]. These dynamic processes are also reflected in the process of transcription, which can display kinetic behavior ranging from isolated uncorrelated events of RNA synthesis to highly cooperative bursts of transcription [5–10]. One way to integrate these molecular events into a coherent view of gene regulation in the

*corresponding author Daniel R. Larson, Dan.larson@nih.gov, 301-496-0986.

Author Manuscript Author Manuscript Author Manuscript Author Manuscript

single cell is to visualize the process of transcription directly through the observation of nascent pre-mRNA synthesis at anactive locus. Here, we describe the implementation of a newly-developed fluctuation analysis approach for quantifying RNA synthesis from a single gene in living cells [7]. The benefit of this method is that it is a direct measure of transcriptional regulation in single cells, independent of upstream steps such as transcription factor binding and downstream steps such as RNA processing and decay.

The approach of observing RNA in living cells was pioneered by Bertrand and Singer and is based on the high-affinity binding of the MS2 bacteriophage coat protein (MCP) to specific RNA hairpins [11] (Fig. 1). Spector and Singer adapted this technique to observe transcription from a reporter gene integrated as a tandem array into the genome [12, 13]. In this implementation, the site of transcription is visible when the fluorescently-labeled coat protein binds the newly-synthesized RNA at the site of transcription. The active transcription site is visible in the microscope as a punctate fluorescent spot in the nucleus against the background of unbound coat protein (Fig. 2). Recently, another coat protein (from the PP7 phage) was also adapted to RNA imaging, extending the combination of labels that can be utilized in any given experiment [7, 14]. Variations on this basic approach have now been used to observe RNA synthesis in real time in living cells of bacteria, yeast, and mammals [15]. These studies differ in the number of insertions observed (array vs. single gene), the coat protein used to visualize the nascent RNA (MS2 or PP7), and the type of analysis for extracting data (FRAP, fluctuation analysis, and others). In this chapter, we focus on one specific implementation: using time-lapse imaging and fluctuation analysis to extract transcription data from single genes.

The guiding principle of fluctuation analysis is that observing the fluctuations of a signal around equilibrium can provide information on the underlying nonequilibrium processes. For example, diffusion is a non-equilibrium process which can be measured by recording fluorescence fluctuations in an optical focal volume in solution [16]. Transport mechanisms of ion channels can be determined by recording the fluctuations in current using electrophysiology [17]. The critical feature of fluctuation analysis is the ability to distinguish the fluctuations of interest (say, those due to a biological process) from other fluctuations which are inevitably present in any experiment. In transcription fluctuation analysis, the fluctuations of interest are due to the biochemical events which control RNA synthesis such as initiation and nascent chain elongation. However, numerous other experimental fluctuations are also present, including noise in photon collection, fluctuations in image analysis, fluctuations in transcription site position, variability in photobleaching, and more. The approach described in this protocol is able to separate the fluctuations due to transcription from the fluctuations due to other sources. In fact, in the case we describe in this protocol for analyzing a single gene, the signal fluctuations are dominated by the events of RNA synthesis. In this regime of one or a few genes, fluctuation analysis is the preferred method for analyzing data. However, in the case of a gene array, the signal shows very little fluctuation, and other techniques such as fluorescence recovery after photobleaching (FRAP) are more appropriate [18].

The protocol is divided into four major steps: 1) reporter gene design, stable cell line construction, and sample preparation; 2) live-cell fluorescence timelapse imaging; 3) image

Author Manuscript Author Manuscript Author Manuscript Author Manuscript

analysis, generation of a transcription time trace, and autocorrelation; 4) data fitting to extract kinetic parameters.

2. Materials

1. Cell chambers with No. 1.5 coverslip at the bottom (e.g. 35mm MaTek, Ashland, MA).
2. Tissue culture plates.
3. Tissue culture reagents: serum, phenol free L15 (used for imaging), DMEM (used for induction and cell culture), Trypsin, 1000× stock concentration of inducer (e.g. Doxycycline) (Sigma Aldrich, St. Louis, MO).
4. Cells co-expressing fluorescently tagged coat protein (MS2 or PP7) and an RNA hairpin cassette.
5. An inverted fluorescence microscope (e.g. AxioObserver, Zeiss, Thornwood, NY).
6. High numerical aperture objective (e.g. Zeiss 63× C-Apochromat).
7. An autofocusing attachment (e.g. Definite Focus, Zeiss, Thornwood, NY)
8. A microscope stage incubator (e.g. Tokai Hit, INUB-LPS, Shizuoka-ken, Japan)
9. A sensitive EMCCD camera (e.g. Evolve 512, Photometrics, Tucson, AZ)
10. A single-line excitation source (e.g. 488nm Excelsior, Spectra Physics, Santa Clara, CA)
11. Optics for separation of excitation and emission (e.g. 488 polychroic beam splitter+ 535/70 nm emission filter, Chroma, Bellows Falls, VT)
12. Image analysis software (custom programs for transcription fluctuation analysis are available at www.larsonlab.net)

3. Methods

3.1 Reporter gene design, stable cell line construction, and sample preparation

1. The first step is preparation of the constructs and stable cell lines. Since these steps are covered extensively in other protocols [10] and vary considerably between applications, we only outline some of the major design considerations in Note 1 and turn now to sample preparation using a standard human cancer cell line U2-OS as an example.
2. Grow the U2-OS cells. Cells are grown in 10 cm tissue culture plates to a density between 20–80%, taking care to keep cells within proscribed passage numbers.
3. Pass cells to microscopy dishes. Trypsinize the cells and place approximately 5,000–10, 000 cells in a 35 mm culture dish with a coverslip affixed to the bottom (see Materials). Total volume in the dish is 2 mL. Note that the thickness of the coverslip on the chamber must match the specifications of the objective.

Author Manuscript Author Manuscript Author Manuscript Author Manuscript

4. Return the cells plated on the microscopy dishes to the incubator under the same conditions as before (media, temperature, CO_2 levels, etc.). Allow the cells to adhere to the bottom of the dish and begin dividing, which usually takes approximately one day. Cells typically grow more slowly on glass than plastic, and some cell lines may not grow at all on microscope coverslips (**see** Note 2).

5. If the reporter gene is inducible, add the inducer and return cells to the incubator. Inducer incubation times vary considerably depending on the reporter gene and the inducible promoter.

6. Switch the cells to Leibovitz L-15 media in preparation for live cell imaging. Leibovitz L-15 is a non-carbonate buffered media designed to optimize cell growth under ambient conditions. Using L-15 eliminates the need to maintain CO_2 partial pressure on the microscope stage, thus substantially simplifying the imaging conditions.

7. If continuing induction is necessary, make sure the imaging media (L-15) contains the inducer (**see** Note 3).

8. Place the microscopy dish on the stage and bring the stage incubator to the correct temperature. Allow the microscope, dish, and stage to thermally equilibrate to minimize drift during the experiment (**see** Note 4). For mammalian cells, the stage incubator is set to 37°C and typically requires at least 15 minutes to equilibrate.

3.2 Live-cell fluorescence timelapse imaging

1. Imaging single molecules of RNA *in vivo* is a demanding application, and care must be taken in the design and operation of the microscope to maximize fluorescence collection and minimize autofluorescence. Several aspects of microscope design are discussed in Note 5.

2. Establish the illumination conditions for the experiment. Excitation power should be set such that the transcription site is readily visible to the naked eye above background but each acquisition does not measurably reduce the fluorescence intensity of the cell. Typical illumination conditions are 0.1 mW of collimated 488 nm light after the objective, resulting in an excitation light intensity in the object plane of 10 mW/mm^2.

3. Establish the exposure time for the acquisition. The exposure time should be long enough that the transcription is visible over the background as shown in Fig. 2. However, the exposure must be short enough to enable imaging at moderate frame rates. Typical exposure time values for the Evolve 512 EMCCD camera are 100 – 200 ms.

4. Establish the *z*-depth acquisition conditions of the experiment. Focus the microscope above and below the transcription site and note the positions. At each time point, the entire *z*-stack will be acquired. For long acquisitions (> 1 hour), there may be some motion in *z*. Taking a larger range of focal positions will ensure that the site does not go out of focus during the acquisition. Typical values

Author Manuscript Author Manuscript Author Manuscript Author Manuscript

are 10 *z*-slices spaced at 0.5 μm, resulting in a total depth of acquisition of 5 μm, which amounts to +/− 2.5 μm above and below the in focus plane of the transcription site.

5. Establish the time-lapse acquisition conditions of the experiment. Images should be acquired at regular time intervals between *z*-stacks. These intervals should capture the transcriptional dynamics being measured while not oversampling the transcriptional state of the cell and causing unnecessary photo bleaching or photo toxicity (**see** Note 6). Typical values are 10 s between *z*-stacks for 512 stacks. Thus, the total number of frames acquired is 5,120 for a total acquisition time of 85 minutes. Under these acquisition conditions, it is possible to resolve both initiation and elongation dynamics (see below).

6. Maintaining focus during the experiment. At each time interval the focus should be adjusted using the autofocus features of the microscope. Specific settings depend on the microscope manufacturer.

3.3 Image analysis, generation of a transcription time trace, and autocorrelation

1. Maximum intensity projection. After images are acquired only the maximum intensity projection of each *z*-stack will be used for subsequent analysis. Maximum intensity projection on three-dimensional image stacks can be performed using any standard image processing software package, for example the freely-available package ImageJ (http://rsbweb.nih.gov/ij/) or FIJI (http://fiji.sc/).

2. Calculate the brightness of the spot at each time point (Fig. 3A). The brightness of the transcription site reflects the amount of RNA present, and the time dependence of this value is the input into the fluctuation analysis procedure. Therefore, this step is critical to correct analysis of the data, and we have developed and tested an algorithm called Localize© which is described in refs ([19–21]) and is available at www.larsonlab.net (**see** Note 7). Briefly, once a time series of projections is produced, each transcription site is identified and fit to a 2D Gaussian on top of a tilted planar background as described in reference (Fig. 3B, C) [7]. The fluorescence intensity of the transcription site is recorded at each time-step as the integrated intensity of the Gaussian fit above the fluorescence background.

3. Construct a trajectory of the transcription site over time. After the brightness and position of the spot have been measured in each frame, the next step is to track the site over time to generate a single time trace for each transcription site. This step is accomplished using a single-particle tracking algorithm developed by Crocker and Weeks [22] and implemented in Localize© which is available at www.larsonlab.net. Briefly, the tracking algorithm uses the coordinates of the spot in one frame to find the nearest neighbor spot in the subsequent frame. By iterative application of this approach, the full time-dependent intensity of the transcription site is generated (**see** Note 8).

Author Manuscript Author Manuscript Author Manuscript Author Manuscript

4. Filling in the gaps in the trajectory. Often, the transcription site disappears, meaning that no nascent RNA is present. This disappearance is expected in the case of single genes which may only transcribe infrequently. The tracking algorithm handles these events by calculating the intensity at the position where the spot was last located. Once the spot reappears, the spot-finding calculation proceeds normally on the newly-visible spot. A full trace is shown in Fig. 3D.

5. The fluorescence intensity time trace is then auto-correlated to a minimum delay time of the imaging interval and a maximum delay time of the total acquisition time. The algorithm used to produce the autocorrelation is based on the multi-tau approach summarized graphically in ref [23]. We have developed an implementation called FCSApp which can be downloaded from www.larsonlab.net. Briefly, autocorrelation with a multi-tau algorithm amounts to multiplying the signal at one point in time by the signal at another point in time at a fixed delay (**see** Note 9). That delay can vary from a lower limit of zero to an upper limit of the length of the experiment. The variable τ is this delay, and $G(\tau)$ is the autocorrelation at each delay (Fig. 3E).

6. Mathematically, the process of computing the autocorrelation is equivalent to:

$$G(\tau) = \frac{< \delta I(t+\tau) \times \delta I(t) >}{< \delta I(t) >^2} \quad (1)$$

where I is the integrated photon number, t is time (in units of the sampling time), and τ is the delay time. $\delta I = I(t) - \langle I(t) \rangle$, where $< >$ denotes the ensemble average.

3.4 Data fitting to extract kinetic parameters

At this point, we emphasize that generation of the autocorrelation curve (section 3.3) from the original raw image data (section 3.2) is primarily a data-processing exercise. No assumptions have been made about the underlying biological processes. In this section, we demonstrate how to fit and interpret transcription autocorrelation curves.

1. Fitting the autocorrelation, $G(\tau)$. It is necessary to first determine which fitting equation applies to the data, based on the experimental design of the reporter construct.

   For constructs with stem loops in the 5' UTR (Fig. 1A), the fitting equation is:

$$G(\tau) = \frac{(T-\tau)}{cT^2} H[T-\tau] \quad (2)$$

   where c is the initiation rate, T is the total dwell time and H is the Heaviside function.

   For constructs with stem loops in the 3' UTR (Fig. 1B), the fitting equation is:

Author Manuscript Author Manuscript Author Manuscript Author Manuscript

$$G(\tau) = \frac{k}{c}\left(\frac{2}{3}\right)\frac{1}{(N(N-1))^2}\sum_{n=0}^{N}(N-n)(N-n-1)(2N+n+1)\frac{(k\tau)^n}{n!} \quad (3)$$

where N is the number of stem loops, τ is the delay time and k is the elongation rate (per stem loop). Note that the number of stem loops N does not appear in the 5' UTR expression (Eq. 2), because in that approximation, the dwell time is dominated by the post-stem loop region.

These closed form analytical solutions can be used to fit the data $G(\tau)$ using standard approaches such as non-linear least squares regression [24]. There are multiple commercial software packages for such fitting, and we use SigmaPlot (http://www.sigmaplot.com/).

2. Interpretation of the autocorrelation fit. The common feature of both fitting equations is the presence of a parameter c which is the initiation rate, and some time parameter which is either the total dwell time of a nascent transcript (T) or the time it takes a polymerase to move between stem loops ($1/k$). The autocorrelation function therefore gives two physical parameters related to transcriptional activity (Fig. 3E) (Note 10).

4. Notes

Note 1:

The system for live-cell RNA visualization relies on two different constructs: the reporter gene which contains the stem loops, and the fluorescently-labeled coat protein which binds the stem loops. We address design considerations for each in turn, starting with the reporter gene.

One must decide how many stem loops are present and where they are located in the construct. Usually, the reporter contains multiple repeats (e.g. 6, 24 or 96) of the stem loop. This multimerization leads to amplification of the signal because each stem loop binds a dimer of the coat protein, and each monomer is labeled with a fluorescent protein (Fig. 1A). Thus, a 24-repeat sequence (length ~ 1.3 kb) can be maximally bound by 48 fluorophores [25]. It is the polymeric feature of RNA which makes it amenable to robust single-molecule imaging. However, the use of 24 stem loops to visualize RNA is slightly a historical artifact: smaller constructs may be visible under optimized microscopy conditions.

The desired position of the stem loops depends on the question of interest. Thus far, the stem loops have been used in un-translated regions of the RNA, for example the 5' and 3' UTRs. Stem loops in the 5' UTR are transcribed first and are therefore retained longer at the site (Fig. 1A). Stem loops in the 3' UTR are transcribed last and have a shorter dwell time at the transcription site (Fig. 1B) [7]. The transcription site of a 5'-labeled gene will appear more often than a 3'-labeled gene because there is a greater probability of observing the nascent transcript (Fig. 1A). The residence time of the 5'-labeled transcript is dominated by the time required for transcriptional elongation (see section 3.4), while the residence time of the 3'-

Author Manuscript Author Manuscript Author Manuscript Author Manuscript

labeled transcript is determined both from elongation and termination rates. Take note that post-transcriptional control sequences are often located in the 3' UTR, so stem loops in this region may perturb, for example, RNA half-lives. On the other hand, stem loops in the 5' UTR may affect translation efficiency.

Transcription site imaging also requires simultaneous expression of the RNA binding protein -- either MS2 or PP7 coat protein -- under control of a constitutive promoter and fused to a fluorescent protein of choice (GFP, YFP or mCherry for example). Achieving the appropriate level of coat protein is critical. Too much, and the transcription site signal cannot be seen over background fluorescence; too little, and the availability of the coat protein may be a limiting factor, leading to dim or invisible transcription sites. The ubiquitin promoter has been used in several studies because it is active in most cell types and expresses at a reasonable level for transcription site imaging [26]. Another variable is the presence or absence of a nuclear localization signal on the coat protein. Many previous studies use coat protein with an NLS, although this signal is not strictly necessary to visualize transcription sites in the nucleus (data not shown).

Note 2:

Some cell lines grow poorly or not at all on glass. One method for improving growth on microscopy dishes is to use the following treatment:

1. 10 minutes in 1 N HCl
2. Remove HCl
3. 2 minutes in 95% ethanol.
4. Rinse three times with sterile PBS.
5. Dish is now ready for cell plating.

Note 3:

The use of inducible promoters is often used to control the expression of the reporter gene. It is important to remember, however, that when measuring transcription in single cells by nascent RNA imaging, one is looking at a snapshot of transcription activity. Care must be taken to ensure the reporter is actively transcribed during the measurement period. Some cell types induce better in certain media or under certain growth conditions which are different from the imaging conditions. Switching media immediately before the experiment may disrupt transcription. Therefore, it is important to probe different environmental conditions. For example, the cells may need to be induced for 24 hours in the Leibovitz L-15 media. Or, conversely, cells may be best induced in DMEM and then switched to L-15 immediately before imaging.

In general, transcription is very sensitive to environmental parameters. Therefore it is necessary to control variability and growth conditions such as cell density, growth rate and induction level.

Author Manuscript Author Manuscript Author Manuscript Author Manuscript

Note 4:

Minimizing experimental drift is a major focus of single-molecule microscopy. In addition to active focus stabilization provided through the microscope, it is important to maintain constant temperature and humidity in the laboratory. In addition, it may be necessary to allow the microscope and the room to thermally equilibrate for many hours under the imaging conditions of the experiment. For example, both the light source and the stage incubator are sources of thermal drift, so it is often beneficial for these instruments to remain on between samples or even imaging sessions.

Note 5:

Single-molecule imaging is a demanding application requiring attention to many details of illumination and excitation. A full discussion is beyond the scope of this protocol, but there are nevertheless several criteria which should be kept in mind. Narrow band excitation (for example using a laser for epifluorescence imaging) maximizes excitation of the fluorophore and minimizes cellular autofluorescence and phototoxicity. High numerical aperture objectives (NA > 1.2) are necessary for efficient photon collection. Electron-multiplying CCDs (EMCCDs) are essential for single-RNA imaging. Excitation and emission filters must be matched to the fluorophore being used in the experiment. The stage incubator must maintain appropriate temperature and humidity levels during the experiment. The above requirements are the ones that are the most difficult to circumvent in single-molecule experiments.

Note 6:

Setting the timescale and imaging parameters is important and also variable for each experiment. Ideally, one should observe a diffraction-limited spot which is visible above the nuclear background (Fig. 2). The fluctuations in brightness reflect the initiation and elongation of RNA, and one should strive to image the spot long enough to observe the spot blinking on and off ~ 5 – 15 times during the course of experiment (Fig. 3D). The excitation intensity and the time series duration may need to be adjusted accordingly. Moreover, the total fluorescence intensity of the cell should not decrease by more than 10% over the course of the experiment.

Note 7:

An object in the light microscope which is smaller than the wavelength of light appears as a diffraction-limited spot or point-spread function [27]. Extracting position information from this point spread function is the subject of numerous papers and is the basis for super-resolution imaging techniques such as PALM [28–30]. In this protocol, however, the spatial information is of incidental importance, while the brightness of the spot is critical. We use a Gaussian mask algorithm described in [20]. This method for calculating the integrated intensity is a hybrid approach where the actual value of each pixel is weighted by the expected value of the pixel given a specific position of the diffraction-limited spot. Therefore, it is a centroid-type approach but with a point-spread function weighting instead of a top-hat function weighting. This algorithm performs well in the low signal to noise regime of the nucleus.

Author Manuscript Author Manuscript Author Manuscript Author Manuscript

Note 8:

There is often only one or zero visible transcription sites in the nucleus, begging the question why it is necessary to track the site over time. In fact, the spot-finding algorithm will also pick up other features such as nucleoli or single RNAs in the nucleus (Fig. 2C). By constructing a trajectory which connects spots found in individual frames, one is effectively applying an additional filter to the data. In other words, the transcription site is allowed to move a proscribed maximum distance between frames. This eliminates the inclusion of spurious spots from other parts of the nucleus which show up during the time series.

Note 9:

The multi-tau algorithm was developed to reduce the error in the correlation at long times. Basically, instead of a single delay bin size (single-tau), the delay bin size width increases with the number of bins. So at long delays (right side of a correlation curve (Fig. 3E)), there are more events in each bin than would have occurred had the bin size remained the same size. The error in multi-tau correlation measurements is discussed in [23].

Note 10:

In a traditional fluorescence correlation spectroscopy measurement, the amplitude of the autocorrelation at a delay time of zero ($G(0)$) is equal to $1/N$, where N is the average number of molecules in the focal volume [16]. In the case of transcription, the interpretation is similar: $G(0)$ is related to the number of transcripts present at the site of transcription. For the 5' UTR, $G(0) = 1/cT$, which is exactly the number of nascent transcripts. For the 3' UTR, $G(0) = (4/3cT)$, which is greater than the number of transcripts. Intuitively, this second relationship derives from the fact that in the case of the 3' UTR, there is a contribution to the autocorrelation from the increase in fluorescence as the stem loops are transcribed (in addition to the total dwell time) which adds to the amplitude. For the 5' UTR, this increase in fluorescence is a negligible part of the time-dependent fluorescent signal and therefore does not contribute to the autocorrelation.

By using these particular models to fit an experimental autocorrelation function, we are making several assumptions about the particular kinetics of transcription initiation and elongation: 1) there are no backward rate constants in initiation or elongation (i.e., once the polymerase starts transcribing, it eventually reaches the end of the gene); 2) the coat protein is not limiting and the on rate is rapid compared to imaging time resolution; 3) single mRNA diffusion in the nucleus is rapid compared to the imaging time resolution. If these assumptions do not apply then other models should be used.

5. Acknowledgement

DRL and MLF are supported by the Intramural Research Program of the NIH, National Cancer Institute, Center for Cancer Research.

7. References

1. Darzacq X, et al., Imaging Transcription in Living Cells. Annual Review of Biophysics, 2009 38: p. 173–196.

Author Manuscript Author Manuscript Author Manuscript Author Manuscript

2. Sinclair P, et al., Dynamic plasticity of large-scale chromatin structure revealed by self-assembly of engineered chromosome regions. The Journal of Cell Biology, 2010 190(5): p. 761–776. [PubMed: 20819934]

3. Neumann FR, et al., Targeted INO80 enhances subnuclear chromatin movement and ectopic homologous recombination. Genes & Development, 2012 26(4): p. 369–383. [PubMed: 22345518]

4. Green EM, et al., A negative feedback loop at the nuclear periphery regulates GAL gene expression. MOLECULAR BIOLOGY OF THE CELL, 2012 23(7): p. 1367–1375. [PubMed: 22323286]

5. Chubb JR, et al., Transcriptional Pulsing of a Developmental Gene. Current Biology, 2006 16(10): p. 1018–1025. [PubMed: 16713960]

6. Golding I, et al., Real-Time Kinetics of Gene Activity in Individual Bacteria. Cell, 2005 123(6): p. 1025–1036. [PubMed: 16360033]

7. Larson DR, et al., Real-Time Observation of Transcription Initiation and Elongation on an Endogenous Yeast Gene. Science, 2011 332(6028): p. 475–478. [PubMed: 21512033]

8. Raj A, et al., Stochastic mRNA Synthesis in Mammalian Cells. PLoS Biol, 2006 4(10): p. e309. [PubMed: 17048983]

9. Zenklusen D, Larson DR, and Singer RH, Single-RNA counting reveals alternative modes of gene expression in yeast. Nat Struct Mol Biol, 2008 15(12): p. 1263–1271. [PubMed: 19011635]

10. Yunger S and Shav-Tal Y, Imaging mRNAs in Living Mammalian Cells, in RNA Detection and Visualization, Gerst JE, Editor 2011, Humana Press p. 249–263.

11. Bertrand E, et al., Localization of ASH1 mRNA Particles in Living Yeast. Mol. Cell, 1998 2(4): p. 437–445. [PubMed: 9809065]

12. Janicki SM, et al., From Silencing to Gene Expression: Real-Time Analysis in Single Cells. Cell, 2004 116(5): p. 683–698. [PubMed: 15006351]

13. Darzacq X, et al., In vivo dynamics of RNA polymerase II transcription. Nat Struct Mol Biol, 2007 14(9): p. 796–806. [PubMed: 17676063]

14. Chao JA, et al., Structural basis for the coevolution of a viral RNA-protein complex. Nat Struct Mol Biol, 2008 15(1): p. 103–105. [PubMed: 18066080]

15. Larson DR, What do expression dynamics tell us about the mechanism of transcription? Current Opinion in Genetics & Development, 2011 21(5): p. 591–599. [PubMed: 21862317]

16. Elson E and Magde D, Fluorescence Correlation Spectroscopy. I. Conceptual Basis and Theory. Biopolymers, 1974 13(1): p. 1–27.

17. Simonneau M, Tauc L, and Baux G, Quantal release of acetylcholine examined by current fluctuation analysis at an identified neuro-neuronal synapse of Aplysia. Proceedings of the National Academy of Sciences, 1980 77(3): p. 1661–1665.

18. Lionnet T, et al., Nuclear physics: quantitative single-cell approaches to nuclear organization and gene expression. Cold Spring Harb Symp Quant Biol, 2010 75: p. 113–26. [PubMed: 21502409]

19. Larson DR, et al., Visualization of retrovirus budding with correlated light and electron microscopy. Proc Natl Acad Sci U S A, 2005 102(43): p. 15453–15458. [PubMed: 16230638]

20. Thompson RE, Larson DR, and Webb WW, Precise nanometer localization analysis for individual fluorescent probes. Biophysical Journal, 2002 82(5): p. 2775–2783. [PubMed: 11964263]

21. Trcek T, et al., Single-mRNA counting using fluorescent in situ hybridization in budding yeast. Nat. Protocols, 2012 7(2): p. 408–419. [PubMed: 22301778]

22. Crocker JC and Grier DG, Methods of digital video microscopy for colloidal studies. J. Colloid Interf. Sci, 1996 179(1): p. 298–310.

23. Wohland T, Rigler R, and Vogel H, The Standard Deviation in Fluorescence Correlation Spectroscopy. Biophys. J, 2001 80(6): p. 2987–2999. [PubMed: 11371471]

24. Bevington PR and Robinson DK, Data reduction and error analysis for the physical sciences1992: WCB McGraw-Hill.

25. Wu B, Jeffrey A Chaoand Singer Robert H., Fluorescence Fluctuation Spectroscopy Enables Quantitative Imaging of Single mRNAs in Living Cells. BIOPHYSICAL JOURNAL, 2012 102(12): p. 2936–2944. [PubMed: 22735544]

26. Lionnet T, et al., A transgenic mouse for in vivo detection of endogenous labeled mRNA. Nat Meth, 2011 8(2): p. 165–170.

Author Manuscript Author Manuscript Author Manuscript Author Manuscript

27. Larson DR, The economy of photons. Nature Methods, 2010 7(5): p. 357–359. [PubMed: 20431547]

28. Betzig E, et al., Imaging Intracellular Fluorescent Proteins at Nanometer Resolution 10.1126/science.1127344. Science, 2006 313(5793): p. 1642–1645. [PubMed: 16902090]

29. Hess ST, Girirajan TPK, and Mason MD, Ultra-high resolution imaging by fluorescence photoactivation localization microscopy. Biophysical Journal, 2006 91(11): p. 4258–4272. [PubMed: 16980368]

30. Rust MJ, Bates M, and Zhuang XW, Sub-diffraction-limit imaging by stochastic optical reconstruction microscopy (STORM). Nature Methods, 2006 3(10): p. 793–795. [PubMed: 16896339]

Author Manuscript Author Manuscript Author Manuscript Author Manuscript

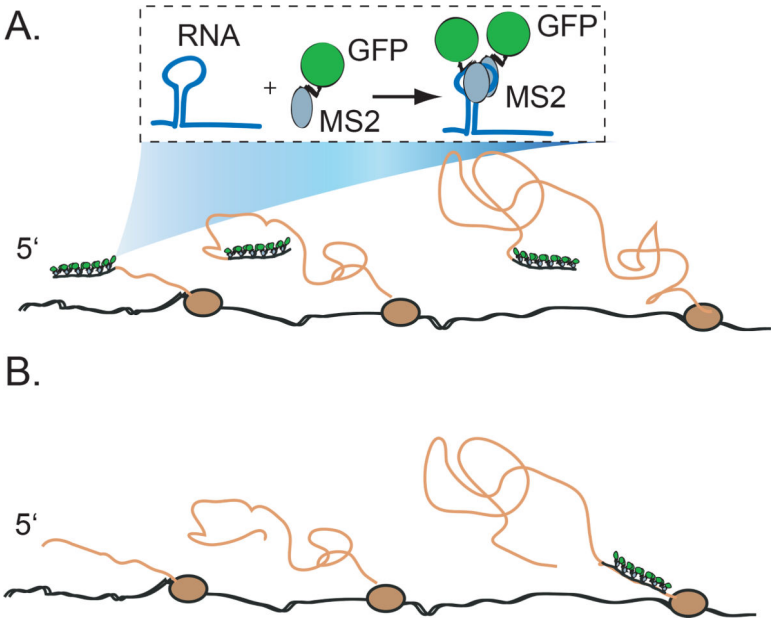

Figure 1.

Scheme for observing nascent RNA in living cells. The approach is based on the high affinity binding of bacteriophage coat protein (i.e. MS2) to hairpins in the nascent RNA. Each stem loop binds a dimer of the coat protein, and each coat protein is labeled with a fluorescent protein (i.e. GFP). **A)** 5’ UTR labeling. When stem loops are located in the 5’ UTR, it is possible to visualize the RNA shortly after elongation commences. Here, three nascent RNAs are visible, resulting in a signal which is three times brighter than a single RNA. **B)** 3’ UTR labeling. When stem loops are located in the 3’ UTR, the nascent RNA is only visible once the polymerase proceeds to the end of the gene. Here, only a single nascent RNA contributes to the fluorescence signal.

Author Manuscript Author Manuscript Author Manuscript Author Manuscript

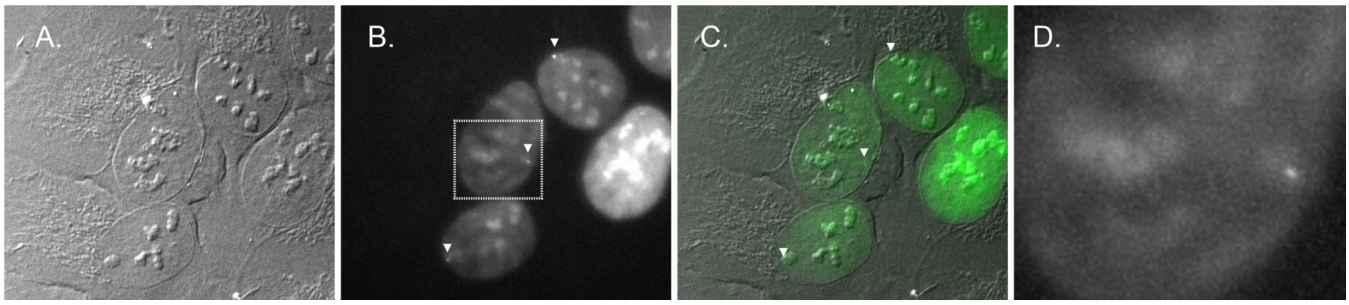

Figure 2.

Visualization of nascent RNA in living cells. **A)** DIC image of U2-OS cells containing a reporter gene inserted randomly into the genome. Nucleoli are visible as dense bodies within the nucleus. **B)** Fluorescence image of PP7-mCherry coat protein with a nuclear localization signal. The coat protein accumulates in the nucleus. The nascent transcription site is visible as a punctate spot (white arrows). At high coat protein expression levels, one frequently observes nucleolus staining as well. The box indicates the region which is magnified in panel D. **C)** Merge of panels A, B. Transcription sites are indicated with white arrows. **D)** Magnification of the demarcated region in panel B. The transcription site is visible near the edge of the nucleus.

Author Manuscript Author Manuscript Author Manuscript Author Manuscript

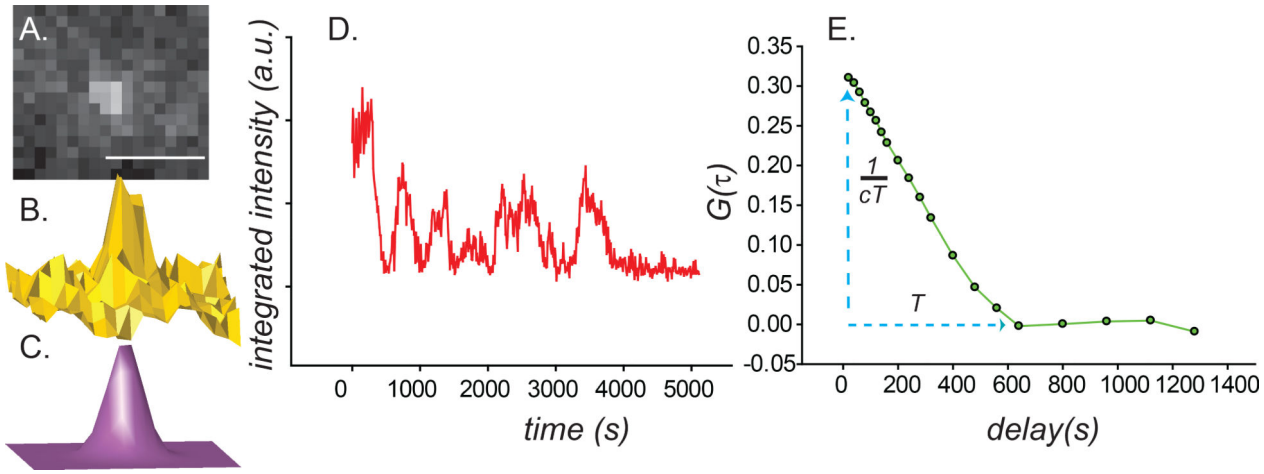

Figure 3.

Fluctuation analysis of transcription activity. **A)** Representative individual fluorescence image from a single transcription site time series. Scale bar = 1.5 μm. **B)** Surface plot of panel A. **C)** Two-dimensional Gaussian fit to the data in panel A. **D)** Transcription site intensity trajectory. Each data point in the curve comes from a determination of spot intensity using the Gaussian mask algorithm. The spot is tracked over many frames, and missing frames are interpolated based on the last known position of the spot. The final output of the tracking program is the fluorescence of the transcription site as a function of time. **E)** Autocorrelation. The time series intensity trajectory is autocorrelated using a multi-tau correlation algorithm. The *x*-axis is the correlation decay; the *y*-axis is the amplitude of the autocorrelation. The fit parameters for the 5' UTR case are shown graphically: the amplitude of the autocorrelation is related to the number of polymerases (cT), and the characteristic decay is related to the dwell time of the polymerase (T).